



# Multi-Stable Stochastic Resonance Model Based on High-Order Time-Delay Feedback Control and Its Application in Weak Signal Detection

---

Wenyue Zhang, Bin Zhang and Yongfei Guo

EasyChair preprints are intended for rapid dissemination of research results and are integrated with the rest of EasyChair.

September 28, 2023

# Multi-stable stochastic resonance model based on high-order time-delay feedback control and its application in weak signal detection

Wenyue Zhang<sup>1\*</sup>, Bin Zhang<sup>1</sup>, Yongfei Guo<sup>1</sup>

<sup>1</sup>Xi'an Jieda Measurement & Control Co., Ltd., Xi'an, Shaanxi 710100, China  
zwy\_ysu@qq.com (FA); zwy\_ysu@qq.com (CA);

**Abstract.** The noise transfer capability of stochastic resonance makes it excellent in the field of weak signal detection. The classic bistable potential well has a simple structure, few parameters and is easy to observe in the physical system, so that a lot of research is carried out based on the bistable stochastic resonance. However, multi-stable potential wells can induce multiple stable responses in nonlinear systems, thereby improving the signal-to-noise ratio(SNR) of the system output signal. In order to break the short-memory effect of the classical stochastic resonance system, a multi-stable stochastic resonance model based on high-order time-delay feedback control(HTFMSR) is proposed in this paper, and it is used for weak signal detection. First, the stochastic resonance effect of the HTFMSR system is demonstrated by deriving the theoretical output SNR. Subsequently, the influence of delay parameters on the system output is studied through the generalized potential function of the system, the steady-state probability density function and the average first transit time. Finally, the weak signal detection ability of the proposed method is verified by two different examples. The experimental results show that the high-order delay feedback item can improve the memory characteristics of the system and improve the signal-to-noise ratio of the output signal of the system.

**Keywords:** Stochastic Resonance, Time-delay Feedback, SNR, MFPT, Weak Signal Detection.

## 1 Introduction

The term "stochastic resonance" was first used by Benzi, Sutera and Vulpiani et al. in the open literature in 1981, and this concept was used to explain the reasons for the periodic changes of the earth's paleoc limate and climate [1-3]. After the concept of stochastic resonance was proposed for the first time, as a separate branch of the nonlinear system discipline, it has received sufficient attention from researchers. The three basic conditions of stochastic resonance include nonlinear system, input signal and noise. In a nonlinear system, the input signal and noise act together to cause the amplification and optimization effect of the system response. The signals collected by sensors usually contain characteristic signals that can reflect the health status of mechanical equipment, as well as interference signals and noise from other coupling components.

Here, signals other than non-characteristic signals can be considered as noise. Therefore, as long as there is a suitable nonlinear system to match the acquisition signal, stochastic resonance can realize weak signal enhancement based on noise utilization, so as to obtain a high signal-to-noise ratio signal containing typical fault characteristics from the acquisition signal. At present, stochastic resonance has been widely used in fault diagnosis of rotating machinery and feature extraction of weak signals[4]. From the perspective of its diagnostic objects, it can be classified into four major categories; bearings [5-7], gears [8-11], rotors [12-15] and others . Because bearings have an extremely critical position in the industry, as many as 60% of the literature researches the method of bearing fault feature enhancement based on stochastic resonance theory.

Early research on SR models primarily focused on classical bistable systems and yielded substantial research outcomes . With the deepening investigation into classical bistable systems, SR models gradually extended to monostable and tristable systems. Zhang et al. introduced an asymmetric time-delay bistable system, analyzing the impact of asymmetric terms and time-delay terms on signal-to-noise ratio and probability density functions. They concluded that time delay could either suppress or promote the occurrence of stochastic resonance phenomena [16]. Gu investigated the time-delay feedback phenomenon in bistable systems with colored noise, analyzing the physical characteristics of the potential function's square term and fourth-order term. They found that delay could significantly enhance the output signal-to-noise ratio. This method can be practically applied in weak signal extraction and recovery domains [17]. Mei et al. derived formulas for signal-to-noise ratio and studied the effect of time delay on stochastic resonance systems with correlated and uncorrelated multiplicative noise and additive noise [18]. Lu et al. proposed a non-stationary weak signal detection strategy based on time-delay feedback stochastic resonance model, demonstrating its suitability for detecting strongly nonlinear non-stationary signals [19]. He et al. discussed stochastic resonance in time-delay bistable systems under Gaussian white noise influence, analyzing the effects of various parameters on average first-passage time, Shannon entropy, and signal-to-noise ratio [20]. Li et al. introduced a weak signal detection approach based on time-delay feedback monostable stochastic resonance (TFMSR) system and adaptive minimum entropy deconvolution (MED), applied to mechanical fault analysis, achieving fault diagnosis for rolling bearings [21]. Shi et al. investigated the dynamical complexity and stochastic resonance of time-delay asymmetric bistable systems, enriching the stochastic resonance model [22]. In fact, the classical stochastic resonance model is a short memory system, and the physical model considering delay is closer to the actual system. However, few studies have focused on the delay in TSR system. At the same time, the stochastic resonance system with a high-order time-delayed feedback has not been studied. Therefore, it is necessary to study the principle of SR based on a high-order time-delayed feedback and its practical value.

This paper proposes a SR system based on a high-order time-delayed feedback and discuss the feasibility of the system for weak fault signature extraction. In section second, derived from the potential function of the system and the stationary probability function. In Section 3, the influence of time delay strength  $\epsilon$  on the mean first-passage

time is analyzed. The influences of  $e$  on the stochastic resonance system from the perspective of the transition of the particles in the potential wells are discussed. In Section 4, the SNR and discuss the effect of the parameters on the SNR are derived. In Section 5, faulty bearing data is dealt with and it is compared with traditional time delay feed back based on tristable stochastic resonance(TFTSR) using the HTFMSR system. At last, Section 6 makes a summary.

## 2 High order time-delay feedback multi-stable stochastic resonance system

The multi-stable Stochastic Resonance (SR) model represents a nonlinear dynamical system subject to both a periodic driving signal and Gaussian white noise. The underlying dynamics of the system can be described by the Langevin equation as follows:

$$\frac{dx}{dt} + \frac{dU(x)}{dt} = A\cos(2\pi ft) + \sqrt{2D}\zeta(t) \quad (1)$$

Where the term  $\sqrt{2D}\zeta(t)$  represents the Gaussian white noise component, the  $D$  denotes the noise intensity.

The multi-stable potential function  $U(x)$  can be formally defined as follows:

$$U(x) = \frac{b}{2}x^2 + \frac{c}{4}x^4 + \frac{d}{6}x^6 \quad (2)$$

Where parameters  $b$ ,  $c$ , and  $d$  are real number.

When a high order time-delay feedback control term is introduced into system, the Langevin equation can be written as follows:

$$\frac{dx}{dt} = -bx - cx^3 - dx^5 + e[x(t - \tau)]^5 + A\cos(2\pi ft) + \sqrt{2D}\xi(t) \quad (3)$$

The HTFMSR system potential function can be written as:

$$U(x) = \frac{b}{2}x^2 + \frac{c}{4}x^4 + \frac{d}{6}x^6 - \frac{1}{6}e[x(t - \tau)]^6 \quad (4)$$

From Eq. (1) and Eq. (2), the Fokker-Planck equation is given by:

$$\frac{\partial p(x, t)}{\partial t} = -\frac{\partial[A(x)P(x, t)]}{\partial x} + \frac{\partial^2[B(x)P(x, t)]}{\partial x^2} \quad (5)$$

Where  $A(x)$  is the conditional mean drift and can be expressed as follows:

$$A(x) = \int_{-\infty}^{+\infty} h(x, x_\tau) P(x_\tau, t - \tau | x, t) dx_\tau \quad (6)$$

$$B(x) = D \quad (7)$$

Where  $x_\tau = x(t - \tau)$ ,  $h(x, x_\tau) = -bx - cx^3 - dx^5 + ex_\tau^5 + A\cos(2\pi ft)$ ,  $P(x_\tau, t - \tau | x, t)$  represents the zeroth-order approximate Markovian transition probability density, which can be expressed as follows:

$$P(x_\tau, t - \tau | x, t) = \frac{1}{\sqrt{4\pi D\tau}} \exp\left(-\frac{(x_\tau^6 - x^6 - h(x)\tau)^2}{4D\tau}\right) \quad (8)$$

Where  $h(x) = -bx - cx^3 - dx^5 + ex^5 + A\cos(2\pi ft)$ .

According to the Markov process, Eq. (6) can be simplified as:

$$A(x) = (1 + 5e\tau x^4)(-bx - cx^3 - dx^5 + ex^5 + A\cos(2\pi ft)) \quad (9)$$

The equivalent Langevin equation for Equation 1 is:

$$\frac{dx}{dt} = (1 + 5e\tau x^4)(-bx - cx^3 - dx^5) + e(1 + 5e\tau x^4)x^5 + (1 + 5e\tau x^4)A\cos(2\pi ft) + \sqrt{2D}\xi(t) \quad (10)$$

By comparing Eq. (10) and Eq. (3), it can be observed that the introduction of a control term  $5e\tau x^4(-bx - cx^3 - dx^5 + ex^5 + A\cos(2\pi ft))$  into the HTFMSR system. This control term incorporates both the effects of delay and feedback, which significantly influence the stochastic resonance output. The resulting generalized function can be expressed as follows:

$$U_e = \frac{1}{2}bx^2 + \frac{1}{4}cx^4 + \frac{1}{6}(d - e + 5e\tau b)x^6 + \frac{5}{8}e\tau cx^8 + \frac{1}{2}e\tau(d - e)x^{10} + (x + e\tau x^5)A\cos(2\pi ft) \quad (11)$$

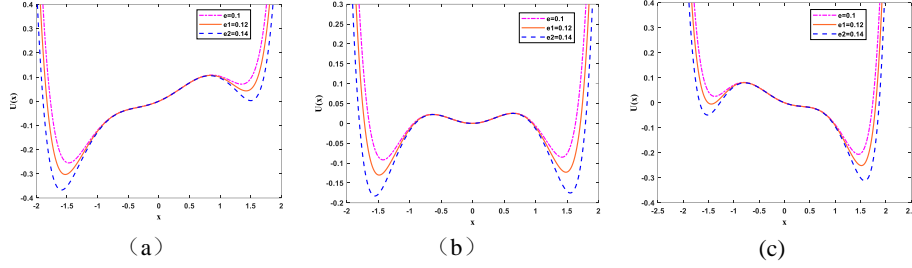


**Fig. 1** The potential function  $U_e(x)$  versus  $x$  for different  $e$  with  $b=0.25$ ,  $c=-0.73$ ,  $d=0.4$ ,  $A=0.2$ , and changes of  $U_e(x)$  at different time (a)  $t=\pi/2$ , (b)  $t=3\pi/4$ , (c)  $t=\pi$ .

The noise-induced escape phenomenon has garnered significant attention in the realm of nonlinear dynamics. The mean first-passage time (MFPT) plays a crucial role as it represents the average time taken for a system to transition from one steady state to another across a barrier. It serves as a valuable descriptor of the transient behavior exhibited by nonlinear systems and forms a fundamental measure in the analysis of escape problems in nonlinear stochastic resonance systems. By employing the definition of mean first-passage time, we can compute the MFPT for two distinct directions within the HTFMSR system, as follows:

$$MFPT(x_{s1} \rightarrow x_{s2}) = \int_{x_{s1}}^{x_{s2}} \frac{dx}{B(x)p_{st}(x)} \int_{-\infty}^x dp_{st}(y) \quad (12)$$

$$= \frac{2\pi}{\sqrt{B(x_{s1})|U''(x_{s1})U''(x_{u1})|^{\frac{1}{2}}}} \exp\left(\frac{U_e(x_{u1}) - U_e(x_{s1})}{D}\right)$$

$$MFPT(x_{s2} \rightarrow x_{s1}) = \int_{x_{s2}}^{x_{s1}} \frac{dx}{B(x)p_{st}(x)} \int_x^{x_{u2}} dp_{st}(y) \quad (13)$$

$$= \frac{2\pi}{\sqrt{B(x_{s2})|U''(x_{s2})U''(x_{u1})|^{\frac{1}{2}}}} \exp\left(\frac{U_e(x_{u1}) - U_e(x_{s2})}{D}\right)$$

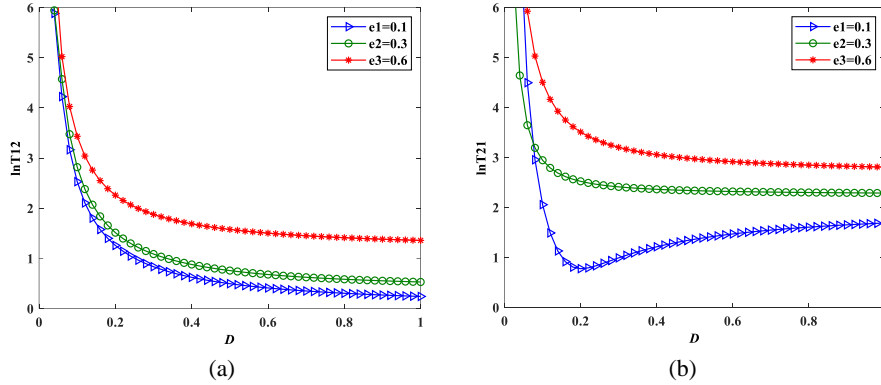


**Fig. 2** The MFPT versus the noise intensity  $D$  for different delay parameters with  $b=0.15$ ,  $c=-0.32$ ,  $d=0.8$ ,  $A=0.2$ ,  $t=\pi/2$ .

By observing Fig. 1(a), it becomes apparent that when  $t=\pi/2$ , the potential function exhibits an asymmetric state. In this state, the left side of the potential function is characterized by lower values, while the right side demonstrates higher values. The disparity in the height of the potential barriers leads to variations in the transit time of Brownian particles within the potential well. Fig. 2 illustrates the MFPT of Brownian particles in two distinct potential wells, considering different time delay strength represented by  $e$ . The results demonstrate that the MFPT exhibits an exponential decay as the noise intensity increases. Furthermore, for the same delay intensity, the MFPT of particles decreases with higher noise intensity, indicating that noise serves as an external stimulus that enhances the transition behavior of Brownian particles. This behavior aligns with the typical stochastic resonance observed in nonlinear systems. Importantly, varying noise intensities exert distinct effects on the particle transition rate. Notably, when the noise intensity  $D = 0.1$ , the transition rate of Brownian particles is maximized, indicating an optimal noise level for the periodic driving HTFMSR system. The time delay intensity  $e$  exerts an influence on the mean first passage time of particles, with the MFPT decreasing as the time delay intensity of the system increases. This observation indicates that an appropriate time delay intensity can effectively enhance the stochastic resonance behavior of the system. Upon comparing Figure 2(a) and Figure 2(b), discernible differences emerge in the MFPT of Brownian particles within the two potential wells. Notably, the transition time required for particles to move from the first potential well to the second potential well is longer than the time taken for the reverse transition. This discrepancy in escape times can be attributed to the dissimilarity in potential barrier heights encountered during the respective transitions. In summary, optimizing the output state of the stochastic resonance system can be accomplished by adjusting the parameters  $e$ , thereby influencing the MFPT of particles within the potential well. Additionally, the escape rate can be enhanced by increasing the intensity of additive noise while accounting for time delay effects.

To provide a comprehensive depiction of the energy distribution of the system's

output signal, the Signal-to-Noise Ratio (SNR) function can be formulated as follows:

$$\begin{aligned}
 SNR &= \frac{\int_0^\infty S_1(\omega) d\omega}{S_2(\omega = 2\pi f)} \\
 &= \frac{-c/8(d-e) - (1/4)\sqrt{b/d-e} - (c + \sqrt{c^2 - 4b(d-e)})/8(d-e)}{c/8(d-e) + (1/4)\sqrt{b/d-e} - (c + \sqrt{c^2 - 4b(d-e)})/8(d-e)} \quad (14) \\
 &\quad \cdot \frac{\pi R_0 A^2 [-c/(d-e) - 2\sqrt{b/(d-e)}]}{4D^2}
 \end{aligned}$$

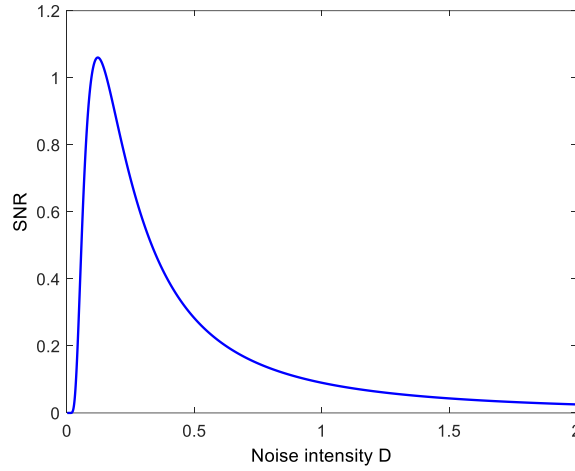


**Fig. 3** SNR versus noise intensity  $D$  with  $b=0.35$ ,  $c=-0.12$ ,  $d=0.9$ ,  $e=0.2$ ,  $\tau=0.2$  and  $A=0.2$ .

Figure 3 illustrates the correlation between the transformed noise intensity and Signal-to-Noise Ratio (SNR). The high-order delayed feedback stochastic resonance exhibits analogous characteristics to classical stochastic resonance: The SNR rises with escalating noise intensity, attains a peak value, and subsequently decreases.

### 3 Weak Fault Signal Detection of Bearing Inner Ring

In this section, we utilize a dataset comprising a set of faults-bearing data provided by CWRU (Case Western Reserve University) to validate the effectiveness of the HTFMSR method for fault diagnosis [49]. Additionally, we compare this method with the traditional multi-stable processing approach. We have previously performed theoretical analyses on HTFMSR systems, it is important to note that the former method must adhere to the adiabatic approximation theory and is confined to small parameter limits. In the case of discrete HTFMSR systems, the output can be computed using the RK4 (Runge-Kutta fourth-order) equation.



**Fig. 4** Test rig

**Table 1.** The main parameters of the rolling bearings.

Inner diameter / mm	Outer diameter / mm	Pitch diameter / mm	Ball diameter / mm	Ball number	contact angle /(°)
25.001	51.999	39.040	7.940	10.000	0

In this research, the fault data is obtained from the Case Western Reserve University (CWRU) Bearing Data Center website. The experimental setup, as illustrated in Figure 4, utilizes deep groove ball bearings of type 6205-2RS JEM SKF operating at a speed of 1730 r/min, with a sampling frequency of 12 kHz. The geometrical details of this bearing type are presented in Table 1, and the corresponding characteristic frequencies are listed in Table 1. For the specific case of inner raceway faults, the theoretical fault frequency of the inner ring is determined to be 156.14 Hz. However, due to the presence of large project-related frequency faults, the small parameter condition is not met. Consequently, a twice sampling frequency transformation method is employed in the data processing algorithm. The twice sampling frequency is set at 6 Hz. Initially, the theoretical fault frequency is considered to be 156.14 Hz.

The frequency spectrum of the inner race fault signal is depicted in Figure 5, revealing a pronounced periodicity in the time domain waveform. Analysis of Figure 5(b) demonstrates that the high-frequency signals predominantly concentrate within the 0-2 kHz range. However, due to substantial background noise interference, it is challenging to extract the fault characteristic frequency from the waveform. Consequently, the proposed method is employed for fault feature detection. In this section, we conduct an analysis and comparison of the potential of the time delay feedback tristable stochastic resonance (TFTSR) system and HTFMSR system in actual fault feature extraction with the following parameter values:  $a=0.1$ ,  $b=-0.2$ ,  $c=$

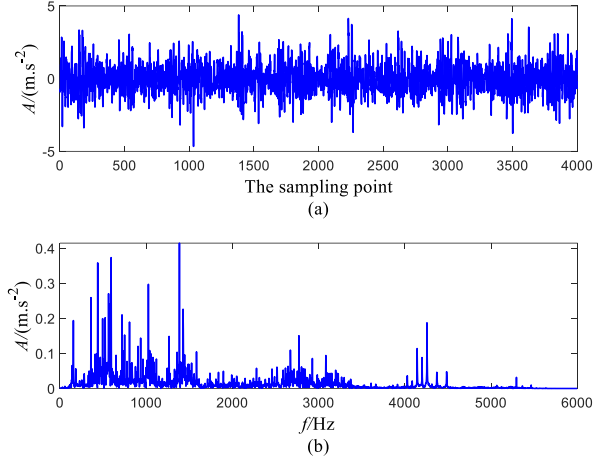


**Fig. 5** Waveform (a) and spectra (b) of a bearing inner ring fault signal

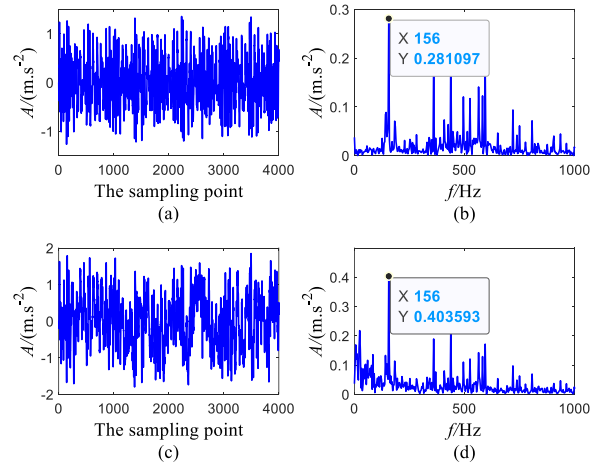


**Fig. 6** Comparison of the waveform and spectra of TFTSR and HTFMSR

0.15,  $e=0.08$ , and  $\tau=0.05$ . As depicted in Figure 5, the original signal is notably susceptible to noise interference. Upon processing the signal using the TFTSR method, as shown in Figure 6 (b), it can be observed that the pulse profile becomes discernible. The filtering process significantly reduces most of the high-frequency interference and also enhances the amplitude of the characteristic frequency. However, some intermediate frequency interference remains, leading to less prominent characteristic frequency peaks. By analyzing Figures 6 (b) and (d), it is determined that the frequency of the inner fault is approximately 156 Hz, which closely aligns with the theoretical value of 156.14 Hz. Comparing the spectra of the TFTSR with the HTFMSR, both methods demonstrate the ability to detect weak fault signals. However, the HTFMSR exhibits a more pronounced filtering effect on the noise interference. HTFMSR system exhibits a higher amplitude at the fault frequency compared to the TFTSR system, increasing from 0.2811 to 0.4036. Furthermore, the signal-to-noise ratio (SNR) analysis indicates

an increase from 0.9723 dB to 2.1840 dB in this processing result. In this section, the fault-bearing data obtained from CWRU is utilized to validate the effectiveness of the HTFMSR method in fault diagnosis. The results demonstrate that the proposed HTFMSR method exhibits superior filtering capabilities compared to the TFTSR method.

In order to quantitatively assess the superiority of the system, faulty bearing data from CWRU is utilized as input. Additionally, the system is driven by noise, and the SNR of both the TFTSR and HTFMSR systems is analyzed to study the impact of noise on the systems. SNR is a critical metric used to quantify the effectiveness of Stochastic Resonance (SR), as it allows for the assessment of the system's ability to distinguish the signal of interest from the background noise.

$$SNR = 10\log_{10}\left(\frac{A_d}{A_n}\right) \quad (10)$$

Where  $A_d$  represents the amplitude value corresponding to the forcing frequency, and  $A_n$  signifies the sum of all amplitude values except  $A_d$  in the amplitude spectrum.

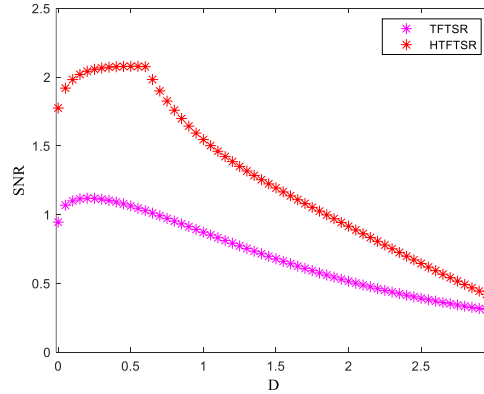


**Fig. 7** The SNR of TFTSR and HTFMSR system

Stochastic resonance is a phenomenon observed in negative feedback systems. In the absence of delay, stochastic resonance relies on the negative feedback provided by the potential trap force within the system. In contrast, delay stochastic resonance incorporates an additional long memory feedback term, which introduces historical information into the current output. Under suitable conditions, this feedback mechanism enables the system to enhance the detection of periodic weak signals, thereby improving the overall detection performance. Figure 7 illustrates the SNR in different systems with noise intensity  $D$ . Notably, the observed trend aligns with the theoretically derived SNR as reported in our previous analysis. It is evident that the HTFMSR system exhibits significantly higher SNR values compared to the TFTSR system. Specifically, the SNR reaches its maximum value of 2.0738 at  $D=0.3$  in the HTFMSR system. Meanwhile, the SNR attains its maximum value of 0.9314 at  $D=0.15$  in the TFTSR system. Further examination of the HTFMSR system indicates that the SNR slowly fluctuates between 2.001 and 2.006 for  $D=0.05-0.6$ , highlighting the system's substantial processing capability within this range of noise intensities. Through a comparative analysis of the signal-to-noise ratios of actual signals, it is evident that the HTFMSR system possesses

superior capacity to transform noise energy into weak signal energy when compared to the TFTSR system, ultimately resulting in an improved amplitude of the fault signal.

Hence, in comparison to the conventional TFTSR system, the HTFMSR system proposed in this study demonstrates enhanced efficacy in extracting weak fault characteristic signals amidst significant noise interference.

## 4 Conclusion

This paper addresses the issue of insufficient detection capability for periodic weak signals in stochastic resonance systems due to their short memory effects. To address this, a multi-stable stochastic resonance model based on high-order time-delay feedback control item is proposed. The incorporation of time-delay feedback control item improves the memory characteristics of the SR model. The research focuses on the generalized potential function, MFPT and SNR of the HTFMSR system. The results indicate that adjusting the time-delay parameter can enhance the transition efficiency of Brownian particles within the potential well, thus improving the system's capability to detect weak signals effectively. In conclusion, the proposed HTFMSR system is validated using a set of publicly available experimental data and is compared with the traditional time-delay feedback stochastic resonance model. The experimental findings demonstrate that the HTFMSR system proposed in this study effectively enhances the detection efficiency of weak periodic signals.

## References

1. Benzi R, Sutera A, Vulpiani A. The Mechanism of Stochastic Resonance[J]. *Journal of Physics A Mathematical & General*, 14(11): 453-457(1981).
2. Benzi R, Parisi G, Sutera A, et al. Stochastic Resonance in Climatic Change[J]. *Tellus*, , 34(1): 10-16(1982).
3. Benzi R, Parisi G, Sutera A, et al. A Theory of Stochastic Resonance in Climatic Change[J]. *SIAM Journal on Applied Mathematics*, 43(3): 565-578(1983).
4. Yang C, Li H K, Cao S X. Unknown Fault Diagnosis of Planetary Gearbox Based on Optimal Rank Nonnegative Matrix Factorization and Improved Stochastic Resonance of Bistable System[J]. *Nonlinear Dynamics*, 111: 1-26(2023).
5. López C, Naranjo Á, Lu S, et al. Hidden Markov Model Based Stochastic Resonance and Its Application to Bearing Fault Diagnosis[J]. *Journal of Sound and Vibration*, 528: 116890(2022).
6. Li G Y, Li J M, Wang S B, et al. Quantitative Evaluation on the Performance and Feature Enhancement of Stochastic Resonance for Bearing Fault Diagnosis[J]. *Mechanical Systems and Signal Processing*, 81: 108-125(2016).
7. He Q B, Wu E H, Pan Y Y. Multi-Scale Stochastic Resonance Spectrogram for Fault Diagnosis of Rolling Element Bearings[J]. *Journal of Sound and Vibration*, 2018, 420: 174-184.
8. Li J M, Wang H, Zhang J F, et al. Impact Fault Detection of Gearbox Based on Variational Mode Decomposition and Coupled Underdamped Stochastic Resonance[J]. *ISA Transactions*, 95: 320-329(2019).

9. Lei Y G, Han D, Lin J, et al. Planetary Gearbox Fault Diagnosis Using an Adaptive Stochastic Resonance Method[J]. *Mechanical Systems and Signal Processing*, 38(1): 113-124(2013).
10. Li Z X, Shi B Q, Ren X P, et al. Research and Application of Weak Fault Diagnosis Method Based on Asymmetric Potential Stochastic Resonance[J]. *Measurement and Control*, 52(5-6): 625-633(2019).
11. Yang C, Li H K, Cao S X. Unknown Fault Diagnosis of Planetary Gearbox Based on Optimal Rank Nonnegative Matrix Factorization and Improved Stochastic Resonance of Bistable System[J]. *Nonlinear Dynamics*, 111: 1-26(2023).
12. Liu Y, Li J T, Feng K P, et al. A Novel Fault Diagnosis Method for Rotor Rub-Impact Based on Nonlinear Output Frequency Response Functions and Stochastic Resonance[J]. *Journal of Sound and Vibration*, 481: 115421(2020).
13. Worden K, Antoniadou I, Marchesiello S, et al. An Illustration of New Methods in Machine Condition Monitoring, Part I: Stochastic Resonance[C]. *Journal of Physics: Conference Series*. IOP Publishing, 842(1): 012058(2017).
14. Qin Y, Zhang Q L, Mao Y F, et al. Vibration Component Separation by Iteratively Using Stochastic Resonance with Different Frequency-Scale Ratios[J]. *Measurement*, 94: 538-553(2016).
15. Lai Z H, Leng Y G. Weak-Signal Detection Based on the Stochastic Resonance of Bistable Duffing Oscillator and Its Application in Incipient Fault Diagnosis[J]. *Mechanical Systems and Signal Processing*, 81: 60-74(2016).
16. Zhang H Q, Xu W, Xu Y, et al. Delay induced transitions in an asymmetry bistable system and stochastic resonance[J]. *Science in China Series G (Physics, Mechanics and Astronomy)*, 53(4): 745-750(2010).
17. Gu X. Stochastic resonance driven by time-delayed feedback in a bistable system with colored noise[J]. *European Physical Journal D*, 66(3): 67(2012).
18. Mei D C, Du L C, Wang C J. The Effects of Time Delay on Stochastic Resonance in a Bistable System with Correlated Noises[J]. *Journal of Statistical Physics*, 137(4): 625-638(2009).
19. Lu S, He Q, Zhang H, Kong F. Enhanced rotating machine fault diagnosis based on time-delayed feedback stochastic resonance[J]. *Journal of Vibration & Acoustics*, 137: 98(2015).
20. He M, Xu W, Sun Z. Dynamical complexity and stochastic resonance in a bistable system with time delay[J]. *Nonlinear Dynamics*, 79(3): 1787-1795(2015).
21. Li J, Li M, Zhang J. Rolling bearing fault diagnosis based on time-delayed feedback monostable stochastic resonance and adaptive minimum entropy deconvolution[J]. *Journal of Sound and Vibration*, 401: 139-151(2017).
22. Shi P M, Xia H F, Han D Y, et al. Dynamical complexity and stochastic resonance in an asymmetry bistable system with time delay[J]. *Chinese Journal of Physics*, 55(1): 133-141(2017).